PROCEEDINGS OF ECOS 2023 - THE 36TH INTERNATIONAL CONFERENCE ON
EFFICIENCY, COST, OPTIMIZATION, SIMULATION AND ENVIRONMENTAL IMPACT OF ENERGY SYSTEMS
25-30 JUNE, 2023, LAS PALMAS DE GRAN CANARIA, SPAIN

Data-driven Modelling of Supermarket Refrigeration Systems for Model Predictive Control Applications

Max Bird[a], Salvador Acha[b], Emilio José Sarabia Escriva[c] and Nilay Shah[d]

[a] *Imperial College London, United Kingdom, max.bird16@imperial.ac.uk, CA*
[b] *Imperial College London, United Kingdom, salvador.acha@imperial.ac.uk*
[c] *Universitat Politècnica de València, Spain, emsaes@upv.edu.es*
[d] *Imperial College London, United Kingdom, n.shah@imperial.ac.uk*

Abstract:
With uncertainty in energy markets, and the effects of climate change looming, reducing energy use and operational cost of existing building systems is more important than ever. To this end, this paper presents a grey-box modelling approach to characterise the behaviour of chilled and frozen and coldrooms using basic system specifications and measured data. An overall energy balance is used to devise a discrete state space model for each cabinet, characterised by unknown empirical parameters relating to heat capacity and heat transfer properties. Historical system data from a UK supermarket are used in combination with a genetic algorithm optimisation to determine the optimal empirical parameters for 10 display cases and 10 coldrooms. The resulting cabinet temperature predictions have a good level of accuracy, achieving a root-mean squared error (RMSE) of 0.37℃ to 0.98℃. Overall this data-driven approach is effective and efficient in modelling refrigeration systems, and can be easily generalised to any system where historical data is available. Finally, the use of the proposed approach in cost minimisation or demand response application is presented.

Keywords:
Supermarket, Refrigeration, Genetic Algorithm, Model Predictive Control, Demand Response

1. Introduction

Commercial refrigeration systems are highly energy intensive and can be responsible for up to 40-60% of a supermarket's overall electricity use [1]. As such, there is clear motivation to reduce energy use and operating costs of such systems through smart control applications. At a high level these control schemes aim to utilise the thermal capacity of refrigerated foodstuffs to shift cooling requirements to low-price or low overall grid demand periods based typically on real-time energy prices to minimise operating costs [2], [3] or demand-side response scenarios [4], [5] to alleviate periods of high grid demand. Such control methods often require simulation models in order to test and calibrate the proposed approach ahead of real-world deployment, which motivates a better understanding of the data requirements and best practices for developing such a model.

A popular refrigeration modelling approach is discussed in [6], which presents 3 separate sub-models to characterise the performance of the chilled cabinets, suction manifold and condenser. A grey-box approach is used to devise the fundamental mass and energy balances across the sub-systems, for which empirical constants are then fit using historical data via an iterative prediction-error minimization (PEM) method. Optimal empirical parameters and temperature fitting results are presented for 7 chilled cabinets, but deliberately excludes behaviour during defrost periods and doesn't consider frozen cabinets. This limits the application of the method to control of real-world systems. An alternative grey-box modelling approach is presented in [7], which uses a state-space model derived from thermodynamic heat and mass balances of individual cabinets and evaporators. Model parameters were estimated using a maximum likelihood estimation approach, based on 2.5 years of minutely telemetry from 6 chilled and 4 frozen units. The approaches lumps the cabinet air and food temperatures together, preventing individual tracking of food temperature which is a key variable to monitor in control applications.

This paper demonstrates a grey-box modelling approach to model temperature dynamics in commercial chilled and frozen cabinets. This is achieved using a genetic algorithm to fit unknown physical parameters for individual cabinets, demonstrated using a UK supermarket as a case study. The method improves over existing literature by modelling temperature dynamics during defrost cycles, as well as explicitly accounting for electric defrost elements present in frozen units.

https://doi.org/10.52202/069564-0069

2. Case Study

2.1. System Description

This paper uses two identical R744 CO_2 booster refrigeration systems installed in a UK food retail store as a case study, shown in Figure 1. Each refrigeration loop services roughly 50% of the cabinets and coldrooms in the store, as detailed in Table 1. They are designed to operate in both the subcritical and transcritical regions depending on the ambient temperatures, but typically they operate subcritically [8]. The flash tank feeds saturated liquid refrigerant to the medium temperature (MT) evaporators in the refrigeration cabinets and coldrooms, as well as feeding the low temperature (LT) evaporators in the frozen cabinets and coldrooms. ”Cabinets” refer to display cases which hold the chilled or frozen food on the shop floor, while ”coldrooms” refer to large rooms in the back of house area which hold additional chilled or frozen stock. Expansion valves are present in each individual cabinet or coldroom, which are locally controlled to maintain the specific cabinet temperature setpoint. A superheat control also operates on the cabinet valves to ensure the refrigerant leaving the evaporators and entering the compressors is only in the gas phase. The LT evaporator outlet feeds directly into the low pressure (LP) compressor bank, and then the MT evaporator outlet mixes with this LP compressor outlet before entering the high pressure (HP) compressor bank. The LP compressor bank is comprised of three 2ESL-4k Bitzer compressors and the HP bank uses six 4FTC-20k Bitzer compressors, one of which has a variable speed drive. The HP compressor outlet then passes through a series of plate heat exchangers which facilitates heat recovery from the refrigeration system into the primary side of the ground-source heat pump (GSHP) which provides heating and hot water services for the building. Refrigerant then enters the gas cooler to remove the remaining heat, the outlet of which feeds the refrigerant flash tank.

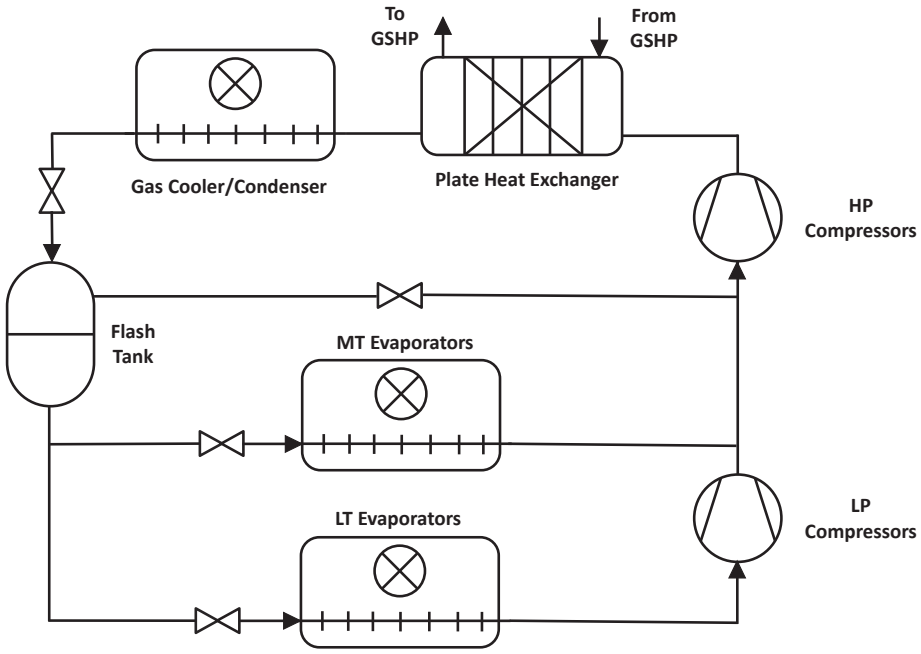

Figure 1: Schematic of typical CO_2 booster refrigeration system.

Due to the subzero refrigerant temperatures required to absorb sufficient heat from the cabinet air, moisture in the air will condense and then freeze over the evaporator. Over time this ice layer can build up and prevent sufficient circulation of the cabinet air which dramatically reduces the available cooling capacity. To prevent this, regular defrost cycles are run in both the LT and MT evaporators. For MT evaporators, an off-cycle defrost is used meaning the refrigerant valve is fully shut for 15-30 minutes, which warms the cabinet and melts the ice, and in LT evaporators an additional heating element is used to actively melt the ice. The operating power of the heating element can be found in the system specification documents for each cabinet. This study is based on data from 10 cabinets (5 chilled, 5 frozen) and 10 coldrooms (5 chilled, 5 frozen) chosen across the two refrigeration systems present in this store.

https://doi.org/10.52202/069564-0069

Fixture	Setpoint [℃]	Refrigeration Load* [kW]	Defrost Power [kW]	System 1 Count	System 2 Count
Fridge Cabinet	1 - 4	2.1 - 7.7	-	36	39
Frozen Cabinet	-20	1.0 - 2.6	5.0 - 21.0	11	12
Fridge Coldroom	1	6.2 - 6.7	-	5	4
Frozen Coldroom	-21	2.6	5.0 - 8.0	3	3

Table 1: Cabinet specifications for each refrigeration system. *Under 25℃ and 60% RH.

2.2. Operating Behaviour

To showcase the operating behaviour of the chilled and frozen cabinets, 12 hours of telemetry data are presented for each cabinet type in Figure 2. All system data are collected using a cloud-based monitoring platform, presented in more detail in [9]. As seen in this plot, the cabinet air temperature is maintained at the setpoint using a local PI controller which manipulates the opening degree (OD) of the expansion valve to provide the required cooling duty. During the off-cycle defrost periods (highlighted in blue) expansion valves fully shut which raises the cabinet air temperature and melts any ice build up. Immediately following the end of the defrost, the valve opens to pull the cabinet temperature back down to setpoint. Frozen cabinet telemetry looks similar but has some notable differences. Firstly, they operate using hysteresis control on the expansion valve, which opens and closes the valve as the cabinet air temperature breaches upper or lower temperature bounds. This control approach is more suitable for frozen cabinets as they use case doors which maintain air temperature much more steadily compared to doorless chilled cabinets. The lack of doors also causes chilled cabinets to need more frequent defrosts compared to frozen units, due to increased ingress of warm, humid air from the shop floor.

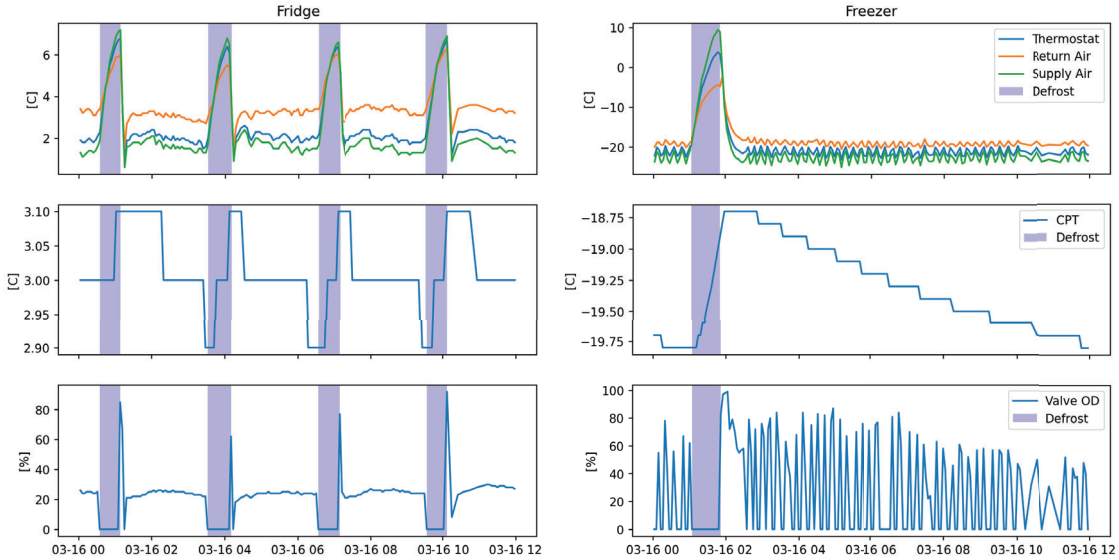

Figure 2: Cabinet telemetry for a chilled cabinet (left) and frozen cabinet (right).

In addition to cabinet air temperature and valve OD sensors, the calculated product temperature (CPT), also referred to as food temperature, in each cabinet is estimated using a proprietary algorithm provided by a resource data management (RDM) panel which monitors and collects data from the local cabinet controllers. As seen in Figure 2, the CPT in chilled cabinets only changes by 0.2℃ during an off-cycle defrost, but can change by up 1℃ during a frozen cabinet defrost due to the additional electric heating element in the evaporator.

3. Modelling

3.1. Cabinet Temperature

The proposed cabinet temperature model is adapted from a popular approach seen in [6], based on an energy balance over an individual cabinet. In cabinets, heat is transferred from the food items to the cabinet air,

https://doi.org/10.52202/069564-0069

$\dot{Q}_{foods/c}$, as well as from the internal building to the cabinet air, $\dot{Q}_{load}$. Heat is then exchanged between the cabinet air and the evaporator, $\dot{Q}_e$. This paper improves upon previous approaches by including the additional term, $\dot{Q}_D$, to account for the heat added by the electrical defrost element present in the evaporators of most frozen units. For all chilled and frozen cabinets, the cabinet air temperature, T_c, and internal building temperature, T_{indoor}, are directly measured using temperature sensors and the calculated product temperature (CPT), T_{food}, is estimated using the previously discussed approach. Assuming purely conductive heat transfer, the energy balance on this system can be written as

$$MCp_{food}\frac{dT_{food}}{dt} = -\dot{Q}_{food/c} \tag{1}$$

$$MCp_c\frac{dT_c}{dt} = \dot{Q}_{load} + \dot{Q}_{food/c} + \dot{Q}_D - \dot{Q}_e \tag{2}$$

$$\dot{Q}_{food/c} = UA_{food}\,(T_{food} - T_c) \tag{3}$$

$$\dot{Q}_{load} = UA_{load}\,(T_{indoor} - T_c) \tag{4}$$

where MCp_{food} and MCp_c are the product of mass and specific heat capacity for the food and cabinet air respectively, and UA_{food} and UA_{load} are the heat transfer coefficients between the cabinet air and the food and store air respectively. The cooling duty of the evaporator can then be written as

$$\dot{Q}_e = \beta\, OD \tag{5}$$

$$\beta = K_v\,(h_{oe} - h_{ie})\,\sqrt{\rho_{suc}\,(P_{rec} - P_{suc})} \tag{6}$$

where OD is the opening degree of the expansion valve, K_v is a valve specific constant, ρ_{suc} is the density of the refrigerant on the suction side, P_{suc} and P_{rec} are the suction and receiver pressures, and h_{oe} and h_{ie} are the specific refrigerant enthalpies at the inlet and outlet of the evaporator respectively. Under normal operation, compressor controllers aim to keep the operating pressures and temperatures of the refrigerant constant at specific points in the cycle, allowing the combination of these parameters into one constant β.

From this point, the above system (1)-(6) can be rearranged and expressed as an LTI state space model.

$$\begin{cases} \dot{\boldsymbol{x}} = A\boldsymbol{x} + B\boldsymbol{u} \\ \boldsymbol{y} = C\boldsymbol{x} \end{cases} \tag{7}$$

with the state values, $\boldsymbol{x} = [T_{food},\, T_c]^T$, controls and disturbances, $\boldsymbol{u} = \left[OD,\, \dot{Q}_D,\, T_{indoor}\right]^T$, and model parameters

$$A = \begin{bmatrix} \frac{-UA_{f/c}}{MCp_f} & \frac{UA_{f/c}}{MCp_f} \\ \frac{UA_{f/c}}{MCp_f} & \frac{-UA_{load}-UA_{f/c}}{MCp_c} \end{bmatrix}, \qquad B = \begin{bmatrix} 0 & 0 & 0 \\ \frac{-\beta}{MCp_c} & \frac{1}{MCp_c} & \frac{UA_{load}}{MCp_c} \end{bmatrix}, \qquad C = \begin{bmatrix} 1 & 1 \end{bmatrix} \tag{8}$$

In order to fit model parameters from historical data, the continuous state space model (7), should be discretised using the sampling time of the sensors.

$$\begin{cases} \dot{\boldsymbol{x}}[k+1] = A_d\boldsymbol{x}[k] + B_d\boldsymbol{u}[k] \\ \boldsymbol{y}[k] = C_d\boldsymbol{x}[k] \end{cases} \tag{9}$$

https://doi.org/10.52202/069564-0069

3.2. Parameter Estimation

The required input data, namely T_{food}, T_c, T_{indoor} and OD are collected for a range of chilled and frozen cabinets from the case study system. An additional binary variable is collected from the cabinet controllers which shows when the cabinet is in defrost mode to allow calculation of $\dot{Q}_D$ using the rated defrost power discussed previously. Raw telemetry is collected at irregular 2-3 minute intervals and resampled to 1 minute intervals using linear interpolation to better capture the dynamics of the system. One day of data from 10/03/2023 is used for each cabinet to show the flexibility of the method using even just a small sample of N total data points. The system (7) - (9) is expressed using the *StateSpace* function within the *scipy.signal* package in Python [10]. This system is then wrapped within a genetic algorithm (GA) optimisation which finds the optimal empirical parameters MCp_{food}, MCp_c, UA_{food}, UA_{load} and β, by using measured system states, $\boldsymbol{x}$ and measured control and disturbances $\boldsymbol{u}$ to estimate the system states in the next timestep $\hat{\boldsymbol{x}}[k+1]$ and compare these to the measured system states $\boldsymbol{x}[k+1]$. This multi-objective optimisation is formulated as

$$\min_{\boldsymbol{Z}} \left(RMSE_c, RMSE_{food}\right) \tag{10}$$

$$RMSE_i = \sqrt{\frac{1}{N}\sum^{N}\left(\hat{T}_i - T_i\right)^2} \tag{11}$$

subject to constraints

$$\begin{cases} \boldsymbol{Z} = [MCp_{food}, MCp_c, UA_{food}, UA_{load}, \beta] \\ \boldsymbol{Z} \geq [0, 0, 0, 0, 10^3] \\ \boldsymbol{Z} \leq [10^9, 10^6, 10^4, 10^4, 10^4] \end{cases} \tag{12}$$

In this paper we utlilise the Python optimisation package *Pymoo* [11] and their implementation of a Non-dominated Sorting Genetic Algorithm (NSGA-II) [12]. Each generation has a population of 100, and the optimisation terminates after 100 generations, and all other GA parameters are left at their default values.

4. Results

The optimal empirical parameters for the chilled and frozen cabinets are shown in Table 1, with *MCp* values given in [J/K], *UA* values in [W/K], β in [W/OD%] and *RMSE* in [K]. For each cabinet, the GA fitting process took at most 2 minutes to complete on a desktop PC with a Ryzen 5 3600 6-core CPU. On average the chilled cabinets have a satisfactory fit, with an RMSE of 0.56℃ and 0.13℃ for cabinet air and food temperature predictions respectively, while frozen cabinets are slightly higher at 0.89℃ and 0.17 ℃ respectively. Chilled cabinets also have higher UA_{load} values, ranging from 42-82 W/K compared to only 1-4 W/K for the frozen cabinets, and higher β values, 3,769 - 6,450 W/OD% compared to 1,000 - 1,576 W/OD% for frozen cabinets. Both of these differences are due to chilled cabinets not having doors, causing a larger heat transfer from the building air to the cabinet air, and consequently requiring a larger evaporator cooling duty to keep the food at setpoint.

	Chilled Cabinets					Frozen Cabinets				
Cabinet ID	1	2	3	4	5	6	7	8	9	10
MCp_{food} ($\times 10^6$)	942.5	222.5	865.8	138.0	951.0	10.7	13.2	577.4	6.3	36.0
MCp_c ($\times 10^5$)	3.2	1.6	2.5	2.2	1.7	2.0	2.1	1.9	1.5	1.8
UA_{load}	82	64	42	60	63	4	3	2	3	1
UA_{food}	391	254	301	222	100	174	189	191	134	194
β ($\times 10^3$)	5738	3796	6450	6308	4673	1576	1050	1000	1050	1032
$RMSE_c$	0.46	0.37	0.68	0.56	0.72	0.98	0.87	0.84	0.89	0.87
$RMSE_{food}$	0.13	0.11	0.15	0.09	0.17	0.18	0.19	0.11	0.18	0.18

Table 2: Empirical parameters and RMSE values for the chilled and frozen cabinets.

Figure 3 shows 24 hours of cabinet air and food temperature predictions from the training sample compared with measured values for the two best chilled and frozen cabinets. Air temperature predictions are generally

https://doi.org/10.52202/069564-0069

good, fitting well the temperature spikes due to defrost, but struggling sometimes to predict the smaller, higher frequency temperature variations when the cabinet is at setpoint. This is particularly noticeable in the frozen cabinet which use hysteresis control to maintain the air temperature within a bound around the setpoint.

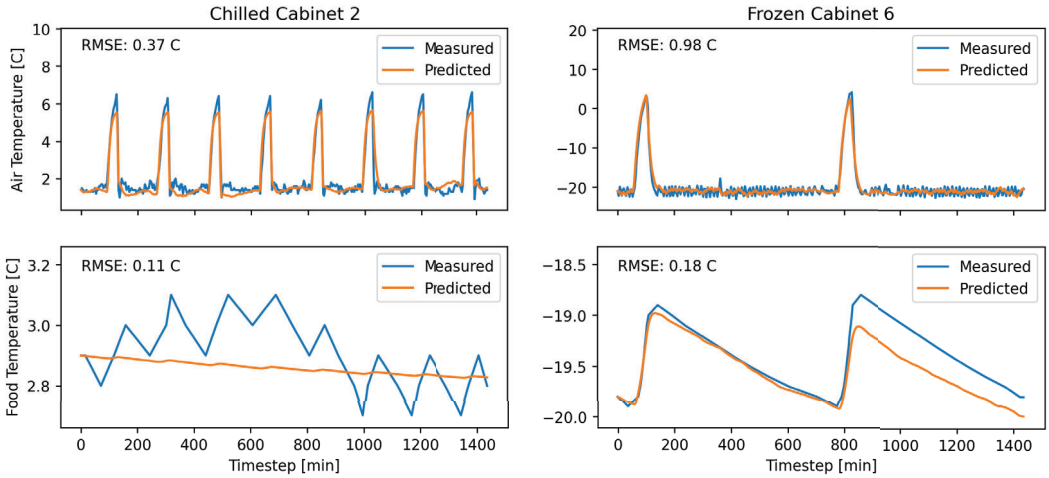

Figure 3: Cabinet temperature predictions based on optimal GA fitting.

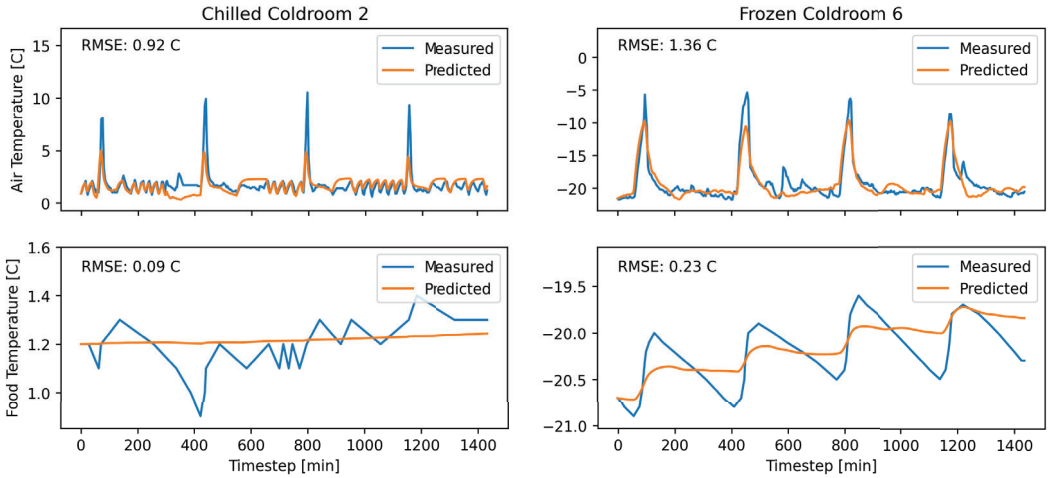

Figure 4: Coldroom temperature predictions based on optimal GA fitting.

Food temperature predictions are less reliable, particularly for the chilled cabinets. Over most of these cabinets the food temperature predictions fail to pick up any of the observed changes in food temperature due to defrost, instead just predicting a constant value which is on average correct. In addition, the food temperature in the chilled cabinets only changes by a maximum of 0.3℃ during a defrost, which is small temperature change for this model to account for, especially compared to the air temperature which varies by around 5℃. Empirical parameters for the 5 chilled and 5 frozen coldrooms analysed can be found in Table 3, and temperature predictions compared to measured values are shown in Figure 4. The air temperature predictions are not as accurate compared to the chilled and frozen cabinets, especially during the defrost periods, achieving an average RMSE of 0.61℃ and 0.16℃ for cabinet air and food temperature predictions respectively for chilled coldrooms, which increases to 2.74℃ and 0.37℃ for frozen coldrooms. This could be due to uneven temperature distribution in coldrooms, which are much larger than cabinets, and so this effect is not by the individual air temperature sensors.

	Chilled Coldrooms					Frozen Coldrooms				
Coldroom ID	1	2	3	4	5	6	7	8	9	10
MCp_{food} ($\times 10^6$)	22.0	799.7	318.6	998.9	997.9	413.0	5.5	15.1	5.2	9.4
MCp_c ($\times 10^5$)	2.3	2.2	10.0	10.0	9.6	0.8	2.7	0.4	0.5	3.0
UA_{load}	15	25	102	111	196	5	27	6	8	75
UA_{food}	241	339	3831	4501	8775	54	178	34	31	251
β ($\times 10^3$)	1000	1002	1706	2964	1054	1000	2631	1811	1355	6121
$RMSE_c$	0.67	0.92	0.29	0.27	0.91	3.07	1.36	3.60	2.73	2.96
$RMSE_{food}$	0.08	0.09	0.14	0.18	0.30	0.26	0.23	0.56	0.31	0.50

Table 3: Empirical parameters and RMSE values for chilled and frozen coldrooms.

5. Application Example

In advanced control applications, simulation models are often required to test and refine the chosen approach prior to real-world implementation. A schematic demonstrating an example framework for a supervisory model predictive control (MPC) approach applied to a refrigeration system can be seen in Figure 5. The MPC scheme will have a user-defined objective function, which is typically minimising operational cost subject to variable electricity prices, or tracking a reference power consumption sent from the grid for demand-response applications. In either case, the key control variable is the optimal temperature setpoint, T^*_{sp}, which can be forwarded to the local cabinet controllers to enact the required expansion valve position *OD*. The devised cabinet models can then be used to simulate the resulting cabinet and food temperature changes. An equivalent modelling and control approach has been demonstrated for a commercial HVAC system in the UK and simulations show the ability to reduce operational costs while adhering to user specified constraints [9].

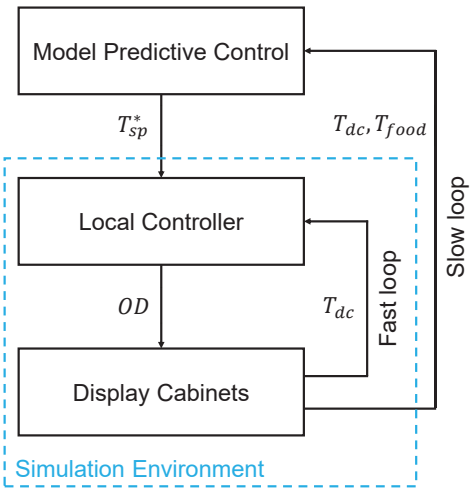

Figure 5: Example supervisory MPC application using refrigeration cabinet model.

The proposed cabinet modelling approach is well suited to these control applications for a number of reasons. Firstly, a large number individual cabinet models can be fit offline with low computational overhead, allowing a user to easily simulate a entire supermarket refrigeration system. Additionally, the modelling approach shows satisfactory modelling accuracy when trained on only a small snapshot of 24 hours of data. Finally, once the optimal empirical parameters are known, the cabinet models are a simple system of linear equations providing a fast, efficient method to test any proposed control approach.

6. Conclusion

This paper presents a data-driven modelling approach to simulate the behaviour of chilled and frozen cabinets and coldrooms, using a UK supermarket as a case study. Individual units are modelled using a discrete LTI state space model, based on an overall system energy balance, for which empirical parameters are determined using a genetic algorithm fitting approach. The proposed approach is demonstrated using 24 hours

https://doi.org/10.52202/069564-0069

of historical data from 10 display cabinets and 10 coldrooms, and shows satisfactory performance across the range of cabinets tested. Finally, a high-level example application of the proposed modelling approach to a supervisory, model predictive control scheme was discussed. Future work should look to better understand the food temperature dynamics, perhaps using temperature probes instead of an estimated CPT value, as this is the most important variable to track in control applications.

Acknowledgments

This research was supported by funds provided via the Imperial College London – Sainsbury's Supermarkets Ltd. Partnership.

Bibliography

[1] Maria Kolokotroni, Zoi Mylona, Judith Evans, et al. "Supermarket Energy Use in the UK". In: *Energy Procedia* 161 (2019). Proceedings of the 2nd International Conference on Sustainable Energy and Resource Use in Food Chains including Workshop on Energy Recovery Conversion and Management;ICSEF 2018, 17 – 19 October 2018, Paphos, Cyprus, pp. 325–332. ISSN: 1876-6102. DOI: https://doi.org/10.1016/j.egypro.2019.02.108. URL: https://www.sciencedirect.com/science/article/pii/S1876610219311907.

[2] Seyed Ehsan Shafiei, Jakob Stoustrup, and Henrik Rasmussen. "A supervisory control approach in economic MPC design for refrigeration systems". In: IEEE Computer Society, 2013, pp. 1565–1570. ISBN: 9783033039629. DOI: 10.23919/ecc.2013.6669413.

[3] "Flexible and cost efficient power consumption using economic MPC a supermarket refrigeration benchmark". In: Institute of Electrical and Electronics Engineers Inc., 2011, pp. 848–854. ISBN: 9781612848006. DOI: 10.1109/CDC.2011.6161162.

[4] Seyed Ehsan Shafiei, Jakob Stoustrup, and Henrik Rasmussen. "Model predictive control for flexible power consumption of large-scale refrigeration systems". In: Institute of Electrical and Electronics Engineers Inc., 2014, pp. 412–417. ISBN: 9781479932726. DOI: 10.1109/ACC.2014.6858921.

[5] Rasmus Pedersen, John Schwensen, Benjamin Biegel, et al. "Aggregation and Control of Supermarket Refrigeration Systems in a Smart Grid". In: *IFAC Proceedings Volumes* 47 (3 2014), pp. 9942–9949. ISSN: 14746670. DOI: 10.3182/20140824-6-ZA-1003.00268.

[6] S. Ehsan Shafiei, Henrik Rasmussen, and Jakob Stoustrup. "Modeling supermarket refrigeration systems for demand-side management". In: *Energies* 6.2 (2013). Cited by: 43; All Open Access, Gold Open Access, Green Open Access, pp. 900–920. DOI: 10.3390/en6020900.

[7] K. Leerbeck, P. Bacher, C. Heerup, et al. "Grey box modeling of supermarket refrigeration cabinets". In: *Energy and AI* 11 (Jan. 2023). ISSN: 26665468. DOI: 10.1016/j.egyai.2022.100211.

[8] Emilio José Sarabia Escriva, Salvador Acha, Niccolo Le Brun, et al. "Modelling of a real CO2 booster installation and evaluation of control strategies for heat recovery applications in supermarkets". In: *International Journal of Refrigeration* 107 (Nov. 2019), pp. 288–300. ISSN: 01407007. DOI: 10.1016/j.ijrefrig.2019.08.005.

[9] Max Bird, Camille Daveau, Edward O'Dwyer, et al. "Real-world implementation and cost of a cloud-based MPC retrofit for HVAC control systems in commercial buildings". In: *Energy and Buildings* (June 2022), p. 112269. ISSN: 03787788. DOI: 10.1016/j.enbuild.2022.112269.

[10] Pauli Virtanen, Ralf Gommers, Travis E. Oliphant, et al. "SciPy 1.0: Fundamental Algorithms for Scientific Computing in Python". In: *Nature Methods* 17 (2020), pp. 261–272. DOI: 10.1038/s41592-019-0686-2.

[11] J. Blank and K. Deb. "pymoo: Multi-Objective Optimization in Python". In: *IEEE Access* 8 (2020), pp. 89497–89509.

[12] K. Deb, A. Pratap, S. Agarwal, et al. "A fast and elitist multiobjective genetic algorithm: NSGA-II". In: *IEEE Transactions on Evolutionary Computation* 6.2 (2002), pp. 182–197. DOI: 10.1109/4235.996017.